TEARING AND KELVIN-HELMHOLTZ INSTABILITIES IN THE HELIOSPHERIC PLASMA

L. Bettarini[(1)], F.A. Rappazzo[(2)], S. Landi[(1)], and M. Velli[(1,3)]

[(1)] *Department of Astronomy and Space Science, Univ. of Firenze, 50125 Firenze, Italy*
[(2)] *Department of Physics, Univ. of Pisa, 56127 Pisa, Italy*
[(3)] *Jet Propulsion Laboratory, California Instiute of Technology, Pasadena 91109, CA*

ABSTRACT

We analyze the magnetohydrodynamic instabilities arising from an initial equilibrium configuration consisting of a plasma jet or wake in the presence of a magnetic field with strong transverse gradients, such as those arising in the solar wind, using 2.5D simulations. Our analysis extends previous results by considering both a force-free equilibrium and a pressure balance condition for a jet in a plasma sheet, and arbitrary angles between the magnetic field and velocity field. The presence of a magnetic field component aligned with the jet/wake destroys the symmetric nature of the fastest growing modes, leading to asymmetrical wake acceleration. Fully 3D simulations are necessary to explore the full dynamics of the instabilities in the generic case.

Key words: Kelvin-Helmholtz – Resistive instability – Slow solar wind – Magnetic Reconnection – Numerical simulation.

1. INTRODUCTION

The evolution of systems consisting in sheared flows in the presence of strong magnetic field gradients poses an important question in plasma physics with applications to magnetohydrodynamic (MHD) structures in several solar and astrophysical environments, such as the interaction of the solar wind with a magnetospheric boundary (**?**), cometary tails (**?**), the heliospheric current sheet (hereafter HCS) (**??**) and solar streamers (**?**).
An MHD model has been developed in which the basic magnetic field is aligned with a fluid jet/wake straddling a neutral sheet (**?**): it accounts, for example, for many of the typical features observed in the slow component of the solar wind. The model has been recently improved by the inclusion of compressibility effects (**?**) as well as those due to curvature in the spherically expanding wind (**??**).
We use a 2.5D MHD code to analyze the stability properties and successive evolution of an initially perturbed equilibrium configuration, consisting in a jet flow (or, equivalently, a wake flow) across which there is a change in initial magnetic field polarity. The angle σ between the asymptotic magnetic field direction and the jet/wake flow is a free parameter: in our simulations we scan different values of σ to explore how it affects the instability properties, properties which also depend on the relative gradients of magnetic field and velocity through the jet.

The primary application we have in mind is solar wind acceleration above helmet streamers, leading to slow solar wind streams where one typically observes a global magnetic field polarity inversion - which may or may not coincide with a ”neutral sheet”. In a reference frame comoving with the slow solar wind, we therefore have a bimodal flow profile where the velocity is zero at the HCS, and across which the interplanetary magnetic field (IMF) changes sign from the Southern to the Northern solar hemispheres, regions of fast wind. Because there are indications (**?**) that the IMF may not go vanish through the sheet, but rotates across something like a force-free configuration (FFC) with a finite, though large, plasma β in the HCS, the instabilities of the combined configuration are non-trivial. Depending on the σvalue there may also be a stabilizing component of the magnetic field along the shear flow. We will consider both an FFC and a simpler model in which the heliospheric current sheet coincides with a neutral sheet and the equilibrium is maintained by a pressure balance condition (PBC).

2. GOVERNING EQUATIONS, PARAMETERS AND INITIAL CONDITIONS

We solve the set of dissipative MHD equations which describe the evolution of a compressible sheared flow in the presence of a strong magnetic field gradient in a Cartesian geometry. We define a *stream-wise* direction (Y) along which we impose periodic boundary conditions and we use fast Fourier transforms to calculate derivatives (**?**); a *cross-stream* direction (X) along which the mean flow varies and we impose nonreflecting boundary conditions using the method of projected characteristics (**???**), adopting a compact finite-difference scheme (**?**), coupled with a hyperbolic tangent mesh stretching around the current sheet; a *span-wise* direction (Z), corresponding to an invariance direction for the quantities describing our system.
Our basic set of equations, written in non–dimensional form, are:

$$\frac{\partial \rho}{\partial t} + \vec{\nabla} \cdot (\rho \vec{v}) = 0 \qquad (1)$$

$$\frac{\partial \vec{v}}{\partial t} + \vec{v} \cdot \vec{\nabla} \vec{v} = -\frac{1}{\rho}\left[\vec{\nabla} P + \frac{|\vec{B}|^2}{2}\right] + \frac{1}{\rho}(\vec{B} \cdot \vec{\nabla})\vec{B} + \frac{1}{\mathcal{R}} \vec{\nabla} \cdot \vec{\zeta} \qquad (2)$$

Proc. Solar Wind 11 – SOHO 16 “Connecting Sun and Heliosphere”, Whistler, Canada
12 – 17 June 2005 (ESA SP-592, September 2005)

$$\frac{\partial \vec{B}}{\partial t} = \vec{\nabla} \times (\vec{v} \times \vec{B}) + \frac{1}{\mathcal{R}_M} \Delta \vec{B} \quad (3)$$

supplemented by the equation of state $P = \rho T$. In the above equations $\rho(\vec{x}, t)$ is the mass density, $\vec{v}(\vec{x}, t)$ is the flow velocity, $P(\vec{x}, t)$ is the thermal pressure, $\vec{B}(\vec{x}, t)$ is the magnetic induction field, $T(\vec{x}, t)$ is the plasma temperature and $\zeta_{ij} = \sigma_{ij} - \frac{2}{3}\,\delta_{ij} \vec{\nabla} \cdot \vec{v}$ is the viscous tensor, where $\sigma_{ij} = \partial_i\, v_j + \partial_j\, v_i$. We have not written the energy equation, since we will assume an isothermal equation of state in most cases. However, in simulations with a pressure-balanced equilibrium, temperature will be allowed to vary across the sheet, and the energy equation in that case is a simple advection equation for temperature, i.e. we will continue to assume $\gamma = 1$.
To render non-dimensional the equations we used the characteristic quantities L^*, v^*, ρ^*, and the related quantities t^*, T^*, B^*

$$t^* = \frac{L^*}{v^*} \qquad T^* = m_p (v^*)^2 \qquad B^* = v^* \sqrt{4\pi\rho^*}$$

where m_p is the proton mass. Both the magnetic resistivity, η, and the shear viscosity, ν, are constant and uniform. The kinetic and magnetic Reynolds numbers are given by $\mathcal{R} = \rho_* v_* L^*/\nu$ and $\mathcal{R}_M = 4\pi v^* L^*/\eta c^2$ respectively. To ensure the solenoidality of the magnetic field and supposing that there is no variation of the fields along z, we introduce the magnetic potential ϕ defined by

$$\vec{B} = \vec{\nabla} \times \left(\phi\, \hat{\vec{e}}_z\right) + B_z \hat{\vec{e}}_z\, .$$

The FFC case consists in the following equilibrium:

$$v_{0y}(x) = \mathrm{sech}\,(x) \quad (4)$$
$$B_{0y}(x) = \mathcal{A}\,[\cos\sigma \mathrm{sech}\,(\delta x) + \sin\sigma \tanh\,(\delta x)] \quad (5)$$
$$B_{0z}(x) = \mathcal{A}\,[-\sin\sigma \mathrm{sech}\,(\delta x) + \cos\sigma \tanh\,(\delta x)] \quad (6)$$
$$T = \frac{1}{\gamma\, \mathcal{M}_S^2} \;\; \rho = 1 \quad \text{(uniform density)} \quad (7)$$

where $\delta = a_V/a_B$ is the ratio between the fluid jet width and the current sheet width; $\mathcal{A}$ and $\mathcal{M}_s$ are respectively the Alfvén number, the ratio between the Alfvén speed and the flow speed, and the sonic Mach number; the angle σ, as already pointed out, defines the initial direction of the asymptotic magnetic field to the basic flow: so if $\sigma = 0$ the asymptotic magnetic field is orthogonal to the velocity field of the fluid jet, except for a "rotation" component in the stream-wise direction, whose intensity depends on to the value of $\mathcal{A}$; if $\sigma = \pi/2$ we observe an almost uniform magnetic field in the negative spanwise direction and the asymptotic magnetic field is parallel to the basic flow through which it changes polarity. By varying the value of σ, we change the initial value of the component of magnetic field along the initial flow and we set the asymptotic magnetic field in an arbitrary direction with respect to the initial velocity field.

In the PBC configuration we consider the following set of functions as basic state:

$$v_{0y}(x) = \mathrm{sech}\,(x) \quad (8)$$
$$\vec{B}_0(x) = \mathcal{A} \tanh(\delta x)[\,\sin(\sigma)\,\hat{\vec{e}}_y + \cos(\sigma)\,\hat{\vec{e}}_z]\,, \quad (9)$$

where the equilibrium is set by a pressure gradient which is on turn assured essentially by a temperature gradient and a constant density. Thus from eq. (**??**) we have

$$T = T_0 + \frac{\mathcal{A}^2}{2} \mathrm{sech}^2(\delta x)\, . \quad (10)$$

In several astrophysical environments the thickness of the neutral sheet is much lower than that of the shear, such as in the case of the interaction between a galactic magnetized wind and a molecular cloud (**?**) as well as in the case of cometary tails (**?**). At 1 AU from the Sun the HCS has a width of about $a_B \sim 10^4$ km ($\sim 6.7 \times 10^{-5}$ AU), while the surrounding plasma sheet is thicker by a factor of 30 (**?**): the parameter δ is much greater than one and it is reasonable to assume that this value does remain high both at large and short distances from the Sun.
Considering the MHD generalization of the Howard semicircle theorem (**??**) it is possible to obtain a critical Alfvénic number, $\mathcal{A}_c$ (**?**), depending on the choice of the parameter δ, below which a system composed by a shear flow and a parallel magnetic field which changes polarity through the jet is unstable only to the hydrodynamic "ideal" modes: the varicose mode, which has a antisymmetric cross-stream perturbed velocity component, and the sinuous mode with the opposite parity. The former has a larger growth rate and both are stabilized for increasing $\mathcal{A}$. Since our purpose is to analyze the dynamical evolution of a strongly magnetized sheared flow we will consider $\mathcal{A} = 1.5$ and $\delta > 5$. In this case, for finite resistivity, only a transverse tearing mode should exist, whose symmetry property is the same of the varicose mode. In general this tearing mode is stabilized for small values of $\mathcal{A}$ and increases linearly with δ (assuming a_V constant).
Numerical simulations performed with $\mathcal{M}_s$ equal about to 1 have not pointed out significant changes in the evolution of the system, so we have chosen the critical value $\mathcal{M}_s = 1$. After several simulations we have decided to assume a value for the Reynolds number such that it is possible to obtain an effective dissipation of energy at the discretization scale and hence we consider $\mathcal{R} = \mathcal{R}_M = 200$. Actually their values are much less than in astrophysical environments, though they are large enough to ensure ideal dynamics at the large scales.
To perturb the initial configuration we consider a white noise in velocity and magnetic potential whose amplitude ϵ is set equal to $\epsilon = 10^{-3}$, allowing development of the linear instabilities without an excessively long transient time. We filter this perturbation by setting to zero all the modes beyond the 20^{th} one. In fact by setting the smallest wave number $s_1 = 0.15$ we consider all the modes

FFC case					
$\lambda = 0.15, \delta = 5, \mathcal{A} = 1.5, \mathcal{M}_S = 1$					
RUN	F0	F1	F2	F3	F4
σ	0	$\pi/8$	$\pi/4$	$3\pi/8$	$\pi/2$

PBC case					
$\lambda = 0.15, \delta = 5, \mathcal{A} = 1.5, \mathcal{M}_S = 1, T_0 = 1$					
RUN	P0	P1	P2	P3	P4
σ	0	$\pi/8$	$\pi/4$	$3\pi/8$	$\pi/2$

Table 1. Table of the simulations and parameters for the solar wind.

in the "window" $\Delta s = 0.15 \div 3$ which includes the values corresponding to the maximum growth rate for both the KH instability and the tearing mode, being the latter ~ 1.3 and the former ~ 0.3, as indicated by the dispersion relation for the FFC case with $\sigma = \pi/2$ (**?**).
We solve the equations in a 2D box, whose length in the stream-wise direction is determine by the smallest wave number, i.e. $\mathcal{L}_y = 2\pi/s$; ϵ is 10^{-3} and always corresponds to the maximum of the function (**??**). In the cross–stream direction the box length is $L_x = 10.63$, this value is the result of the mesh stretching. In the simulation that we present, we use a numerical grid with $n_x \times n_y = 361 \times 128$.

3. RESULTS OF NUMERICAL SIMULATIONS

Table (**??** summarizes all the simulations performed to study how the relative directions between the basic magnetic and sheared velocity field affects the stability properties of the system. In the case of $\sigma = 0$, the system

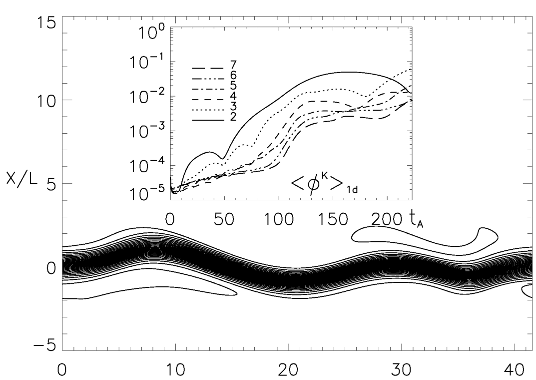

Figure 1. Contour of the magnetic potential at the instant $t = 200$ for F0: it is possible to observe the system is still slightly perturbed. In the small window we show the plot of its first seven instability modes: the growth rate of the 2^{nd} mode, the fastest one corresponding to $s = 0.3$, is about $\Gamma \sim 0.05$.

shows the typical Kelvin–Helmholtz sinuous evolution for both pressure balanced and force-free configurations. For the run P0 we observe a more rapid instability with a growth rate of $\Gamma \sim 0.09$ corresponding to the fastest mode whose wave number is $s = 0.75$. In Fig. **??** we show the magnetic potential contour for $t = 200$ and its first seven modes for the run F0: we observe that there isn't a clear linear regime, but an initial stable phase with a successive "almost-linear" instability evolution where it is possible to note fast coupling between the larger wavelength modes (the mode 2, corresponding to $s = 0.3$, has a growth rate of ~ 0.05), followed in turn by an increase of the sinuous behavior. In the latter configuration a more effective acceleration of the solar wind wake is produced: at $t_A \sim 160$ we have that $\Delta v_{pbc} \sim 0.55$ instead of $\Delta v_{ffc} \sim 0.25$ for the FFC case. During the instability evolution the system maintains in both cases its initial symmetry property.
In general for $\sigma > 0$ we observe, for both kinds of equilibrium configurations, that in the nonlinear regime the flow shows a resistive-varicose evolution triggered by a reconnection process with a consequent magnetic coalescence behavior. In the FFC case depending on the value of σ the jet undergoes a deceleration which is not symmetric with respect the stream-wise direction. In fact for different values of σ we have a different profile for the magnetic potential that produces a shift of the current sheet with respect the jet/wake symmetry axis. This loss of symmetry in the evolution of the system produces also a preferential side of the sheet where the magnetic islands originate during the the reconnection process of the nonlinear regime: in Fig. **??** it is possible to observe the contour of the magnetic potential at the begin of the nonlinear regime ($t \sim 70$) where the closed magnetic structures are originating on one side of the current sheet. In the small plot we observe the profile of the stream-wise velocity component for different instants: we obtain a strong but asymmetric deceleration of the jet. For the PBC case we have the same deceleration of the jet, but no shift is observed, due to the symmetry of the basic system despite the value of σ. In general the linear growth rate increases with the value of σ and it is larger for the PBC case than the FFC one for all the configurations, except $\sigma = \pi/2$. This is due to the configuration of the force-free field: in fact this produces a stabilizing magnetic field stream-wise component which is stronger for small values of σ, that is $B_{0y}^{FFC}(\sigma \sim 0) \sim \mathcal{A}(1 - \sigma^2/2)$, while in the PBC case we have $B_{0y}^{PBC}(\sigma \sim 0) \sim 0$.

4. CONCLUSIONS

By observing the evolution of a sheared flow in the presence of a strong magnetic field gradient we can make a few considerations about the dynamic properties of a magnetically dominated fluid system, in which it is possible to observe a generic inclination between the velocity and the magnetic field, like the wake configuration of the solar wind beyond the first 15-20 solar radii. Irrespective of the nature of the equilibrium, be it a force-free or a pressure balance configuration, there is always a tearing process which destroys the natural magnetic field stabilization property, therefore triggering the evo-

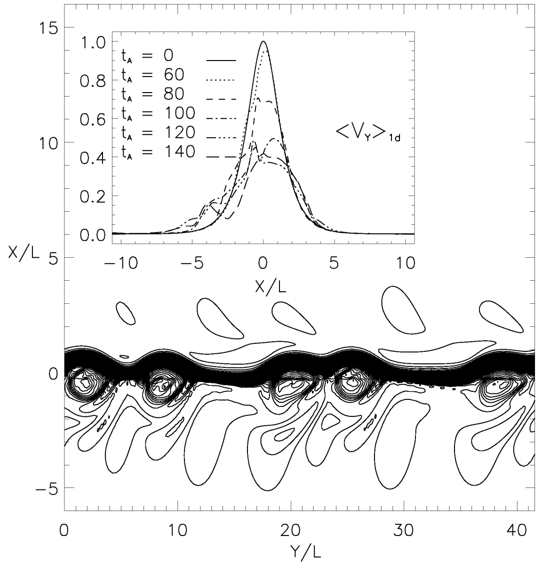

Figure 2. Magnetic potential contour at $t \sim 70$ for F1, which shows the preferential side of the current sheet where magnetic islands originate. In the small plot we can observe the stream-wise velocity component of the jet for different instants for the same run: the deceleration is antisymmetric due to the shift of the current sheet with respect to the wake symmetry axis.

lution of a Kelvin-Helmholtz type instability. This leads to a varicose-resistive evolution because we are in a magnetically dominated regime. For the FFC configuration by increasing the angle σ the intensity of the stabilizing stream-wise component of the magnetic field decreases and this allows a faster linear regime of the instability. This process produces a deceleration of an embedded jet or alternatively to the acceleration of the central part of a wake: for the FFC case this process is not symmetric with respect the stream-wise direction: the initial magnetic field configuration for $\sigma \neq 0, \pi/2$ does not have a defined parity with respect to the velocity stream extrema. In order to analyze the behavior of the modes with the angle σ and so to study the exact evolution of the system we have to do a fine tuning of the white noise amplitude to avoid as much as possible the initial couplings between the modes, above all the lower ones, which alter the linear regime and the successive evolution of the system. The configurations presented here, with arbitrary angles of magnetic and velocity field, also require fully 3D simulations to completely explore the unstable phase-space. Such simulations are presently being carried out.

ACKNOWLEDGEMENTS

We thank Andrea Verdini for the useful discussions. This work was completed while the authors were participating in the NSF funded IPAM program “Grand Challenge Problems in Computational Astrophysics” at UCLA. This work has also been partially supported by tthe Research Training Network (RTN) Theory, Observation, and Simulation of Turbulence in Space Plasmas, funded by the European Commission (contract HPRN-CT-2001-00310). MV acknowldeges support from NASA.

REFERENCES

Cravens, T. E. 1997, The physics of the solar system plasmas (Cambridge University Press)

Dahlburg, R. B., Boncinelli, P., & Einaudi, G. 1998, Phys. of Plasmas, 5, 79

Drazin, P. & Reid, W. 1981, Hydrodynamic stability (Cambridge University Press)

Einaudi, G., Boncinelli, P., Dahlburg, R. B., & Karpen, J. T. 1999, J. Geophys. Res. A, 104, 521

Einaudi, G., Chibbaro, S., Dahlburg, R. B., & Velli, M. 2001, Astrophys. J., 547, 1167

Frigo, M. & Johnson, S. G. 1998, in Proc. 1998 IEEE Intl. Conf. Acoustics Speech and Signal Processing, Vol. 3 (IEEE), 1381–1384

Howard, L. N. 1961, Journal of Fluid Mechanics, 10, 509

Jeffrey, A. 1969, Magnetohydrodynamics (Oliver & Boyd)

Lele, L. K. 1992, J. Comp. Phys., 103, 16

Opher, M., Liewer, P. C., Velli, M., et al. 2004, Astrophys. J., 611, 575

Rappazzo, A. F., Velli, M., Einaudi, G., & Dahlburg, R. B. 2003, in AIP Conf. Proc. 679: Solar Wind Ten, 371–374

Rappazzo, A. F., Velli, M., Einaudi, G., & Dahlburg, R. B. 2005, Astrophys. J.

Roe, P. L. & S., B. D. 1996, SIAM J. Appl. Math., 56, 57

Shore, S. N. & Larosa, T. N. 1999, Astrophys. J., 521, 587

Slavin, J. A., Smith, E. J., Tsurutani, B. T., et al. 1986, Geophys. Res. Letts., 13, 283

Smith, E. J. 2001, J. Geophys. Res. A, 106, 15819

Uberoi, C. 1984, J. Geophys. Res. A, 89, 5652

Vanajakshi, T. C., Thompson, K. W., & Black, D. C. 1989, Journal of Comp. Phys, 84, 343

Wang, S., Lee, L. C., Wei, C. Q., & Akasofu, S.-I. 1988, Solar Phys., 117, 157